Narodowe Centrum Badań Jądrowych

RAPORT NCBJ CIŚ Nr B –..2../2015

Title: Hydraulic divider geometry optimization with the use of CFD analysis tools.

AUTORS: D.Zgorzelski, P.Prusiński, T.Kwiatkowski, S.Kozioł

Abstract:

Since 2012, National Centre for Nuclear Research in Poland is constructing its own Data Centre for HPC under the name Świerk Computing Centre (CIŚ). It will be ready in 2015 reaching its target - 500 TFLOPS. One of its major current problems is the unstable work of HPC cluster cooling system, resulting in the increase of the maintenance costs. The main aim of this work is to investigate this problem with use of the Computational Fluid Dynamics (CFD) code. The investigation is focused on the system part called fluid divider that is suspected to be a source of unstable system operation. In this paper, wide range of cases will be analysed, covering different work regimes of the installation and various geometry modifications. Finally, certain improvement in the current design will be suggested by the CFD Analysis Group.

Conducted in:

Świerk Computing Centre (CIŚ).

Date: 03.02.2015

Zatwierdzam do użytku służbowego:

Zastępca Dyrektora
Narodowego Centrum Badań Jądrowych
ds. Infrastruktury Badawczej
prof. dr hab. Krzysztof Wieteska

Data: **Dyrektor**

Nr tematu, zadania zlec.	Symbol UKD	Symbol INIS
....		

RAPORT NCBJ CIŚ Nr B –2/2015

Title: Hydraulic divider geometry optimization with the use of CFD analysis tools.

AUTORS: D.Zgorzelski, P.Prusiński, T.Kwiatkowski, S.Kozioł

Abstract:

Since 2012, National Centre for Nuclear Research in Poland is constructing its own Data Centre for HPC under the name Świerk Computing Centre (CIŚ). It will be ready in 2015 reaching its target - 500 TFLOPS. One of its major current problems is the unstable work of HPC cluster cooling system, resulting in the increase of the maintenance costs. The main aim of this work is to investigate this problem with use of the Computational Fluid Dynamics (CFD) code. The investigation is focused on the system part called fluid divider that is suspected to be a source of unstable system operation. In this paper, wide range of cases will be analysed, covering different work regimes of the installation and various geometry modifications. Finally, certain improvement in the current design will be suggested by the CFD Analysis Group.

Conducted in:

Świerk Computing Centre (CIŚ).

Date: 03.02.2015

Zatwierdzam do użytku służbowego:

....

Data: **Dyrektor**

Nr tematu, zadania zlec.	Symbol UKD	Symbol INIS
………………		

Contents

1. Introduction

Nowadays, progress in almost any field of research, especially in engineering sciences, often depends on development and access to High Performance Computing (HPC) facilities. Fortunately, a number of such computing or data centres is still growing.

Since 2012, National Centre for Nuclear Research in Poland is constructing its own Data Centre for HPC under the name Świerk Computing Centre (CIŚ) in a framework of EU grant no. POIG.02.03.00-00-013/09. This installation will be ready in 2015 reaching its target - 500 TFLOPS.

One of its major current problems is the unstable work of HPC cluster cooling system which is the reason of the increased maintenance costs due to extensive exploitation of the cooling chillers. Observed instabilities are caused by the fluid oscillations occurred in the interior of the fluid divider. The main aim of this work is to investigate this problem thoroughly and propose the solution that fix it by the means of Computational Fluid Dynamics (CFD) technique.

The CFD allows the user to get an insight into the industrial processes engaging mass and energy transfer with a high resolution even if the experimental setup is a kind a black box like in this case. All these help to track physical phenomena in a very local scale and in turn helps to keep the installation both in its optimal/safe or maximum performance conditions depending on needs.

In the following chapters, one information on the HPC and its cooling systems with a special focus on a part commonly called fluid divider that is suspected to be a source of unstable system operation is included. In the next chapters, CFD model with a consideration related to domain discretisation and assumptions to be made will be presented together with a wide range of cases covering different work regimes of the installation. Afterwards, a new design proposed by CFD Analysis Group will be discussed. Finally, the modifications in the current design will be suggested.

2. Cooling infrastructure - problem definition

Investigated cooling system has been designed to provide up to the 1 600 kW of the cooling power. The installation consists of two heat exchangers 800 kW each, that are connected to 5 chillers of about 400 kW each. One chiller is redundant so the total cooling capacity reaches 1 600 kW. Chilled water is devoted to cool the HPC cluster, which can generate up to 1 600 kW of heat divided into 4 rows of rack boxes.

However, only two from four chillers and one row of rack boxes are installed by now. Current electric power maximal load of the computational part of the infrastructure is about 300 kW, with 400 kW of total cooling capacity. The scheme of the entire analysed installation is shown on Fig 1:

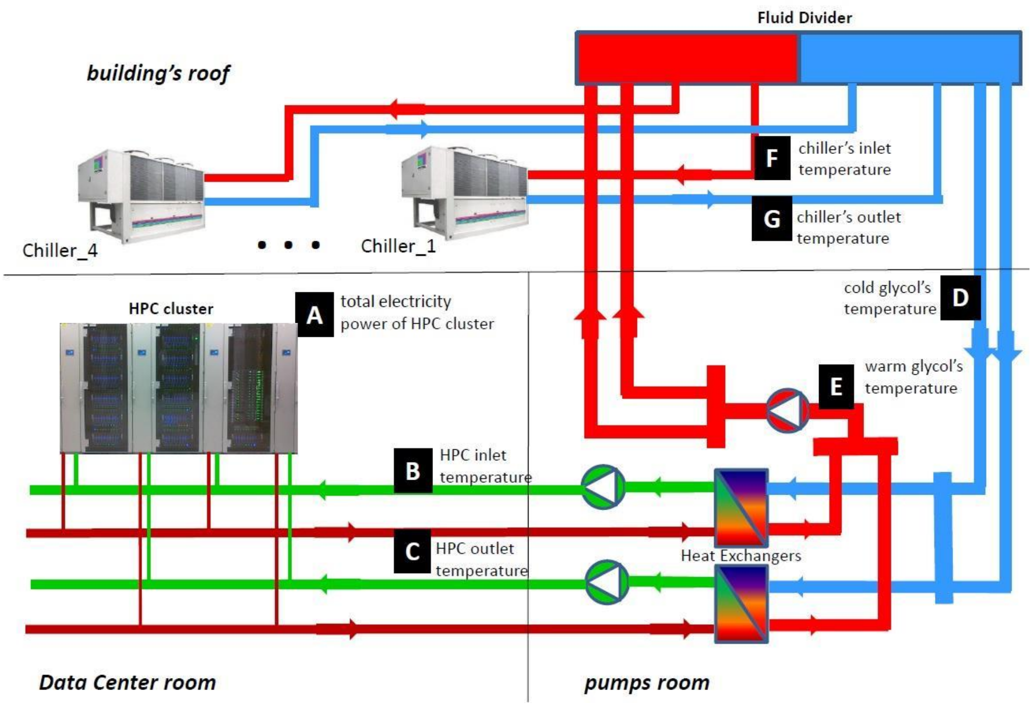

Fig. 1. Scheme of the current cooling installation.

The chillers are placed on a building roof, each of them is equipped with two inverter pumps, five scroll compressors and integrated free-cooling option. They are installed in glycol's part of the cooling system. The heat from the data centre room is transferred to the system through two heat exchangers, while pumps A and B provide water circulation there.

Under the constant cooling conditions, the system is supposed to work stable, but it does not. The evidence of the unstable work can be found in figure 2, where cold glycol's temperature (plot D) starts to oscillate despite the constant or almost constant total electricity power of HPC cluster (plot A) (i.e. 6 A.M. - 8 A.M. and 12 P.M. - 14 P.M.).

As a result of that, chillers' controllers start to turn on and off selected compressors alternately. It causes an increase in power consumption compared to the similar, but constant work of chillers. This abnormal measurements are depicted in figure 3.

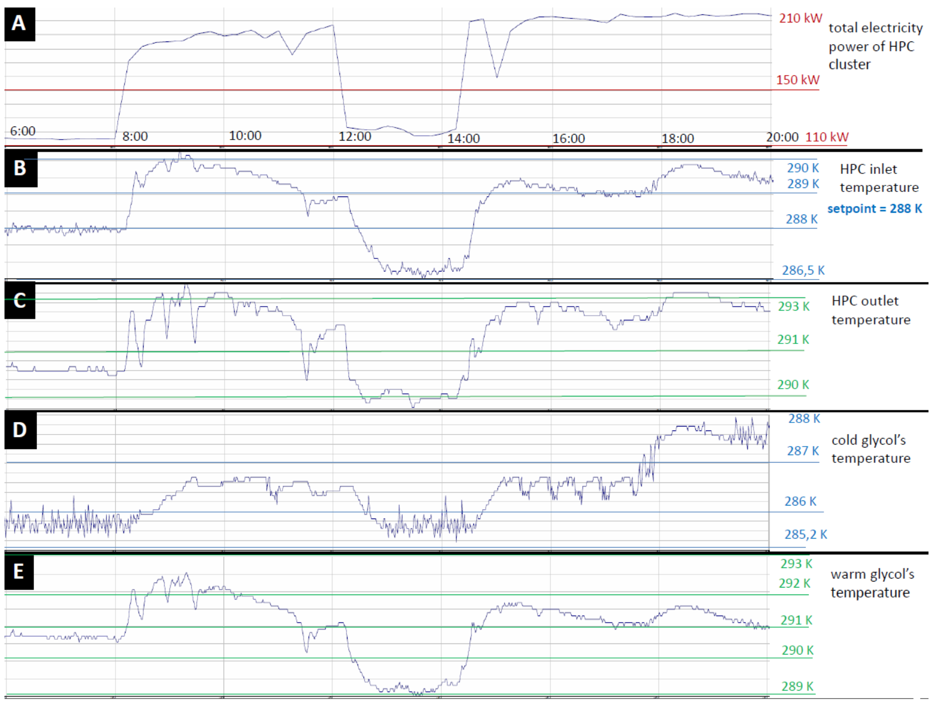

Fig. 2. Temperature on selected measurement points and total electricity power of HPC.

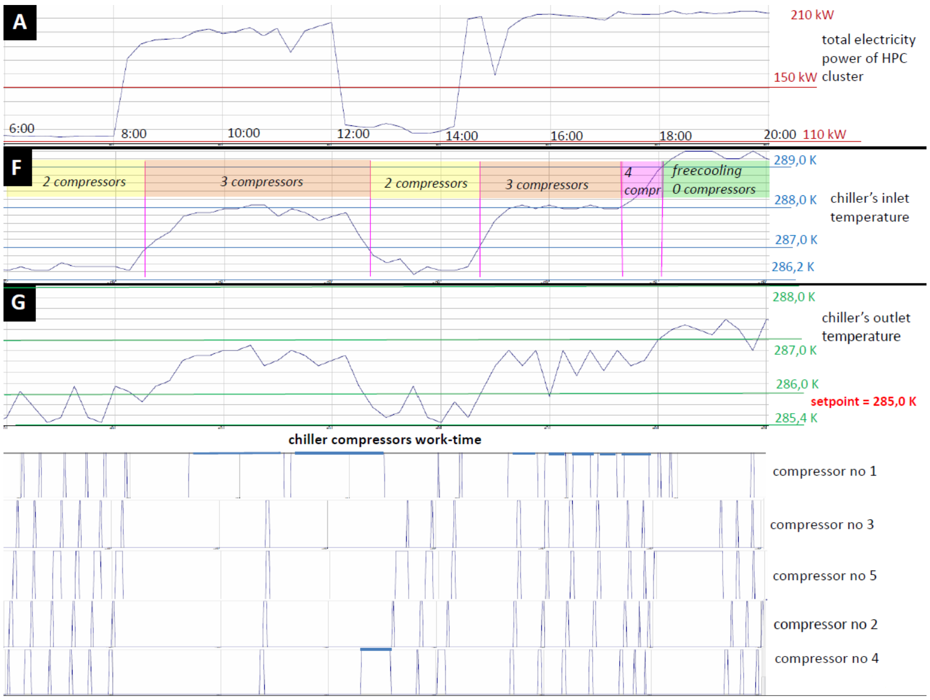

Fig. 3. Total electricity power and compressors working.

Moreover, chillers have been examined thoroughly by authorized specialists who proved their proper work. Thus the fluid-divider is suspected, to be a source of glycol's temperature oscillations. Unfortunately, the fluid divider is in essence a kind of a "black-box", with no viewfinder and just two thermocouples sampling data with a low frequency from the volume of over 0.85 m^3. To prove these claims and to examine the fluid-divider, CFD simulation seems to be the only technique to be used in this case.

3. Simulation of the current fluid divider

The fluid divider is an external component of computer cluster cooling system that joints primary circuit with chiller-fans circuit. Assuming the hydraulic divider has to be treated as a black box, a numerical simulation became the only way to examine fluid flow inside the divider. Then the investigation may show possible anomalies in the work of considered system. In order to perform this type of analysis in the CFD code, the geometry, mesh and appropriate CFD model should be created and discussed.

The whole process of modelling was conducted using ANSYS Workbench 15.0. Geometry was modelled in Design Modeler, mesh was created in the Meshing module and simulations were performed in the Fluent.

3.1 Geometry

The examined geometry consists of the cylindrical collector with a set of inlets and outlets. In the figure 4 the scheme of this device is presented. Starting from the left hand side of the scheme, there are two inlets from pumps A and B or to be more precise from pump sections A and B, subsequently four outlets to chillers (chiller 1, 2, 3 and 4_5 - chiller 4_5 is a double chiller), next four chiller inlets and at the end, two outlets to the pumps (rotated by 90 degrees).

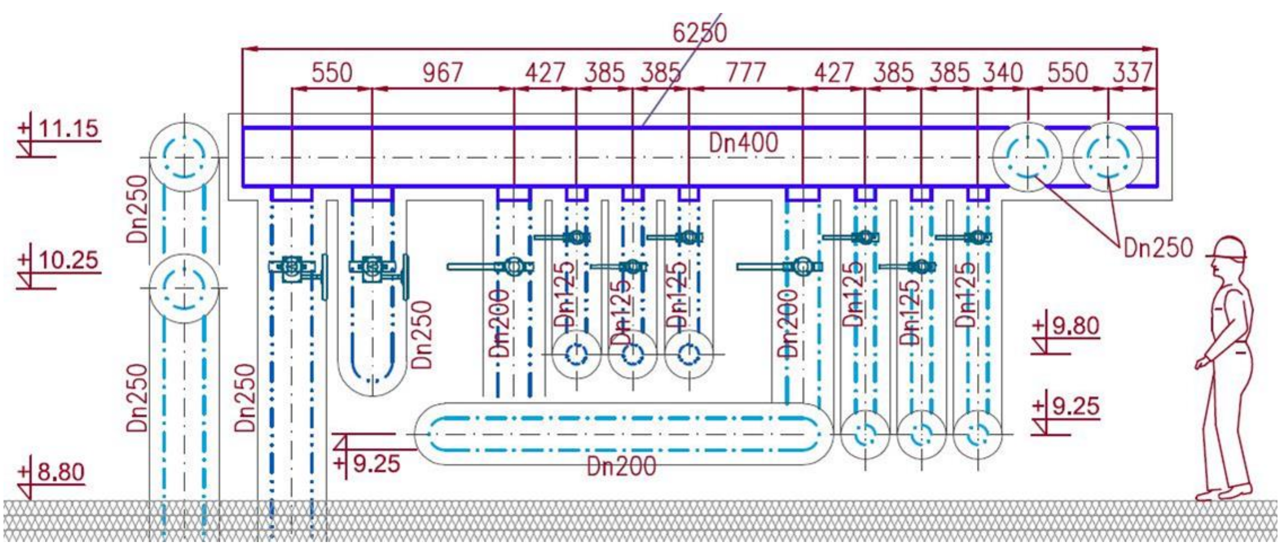

Fig. 4. Dimensions of the fluid divider.

Usually, only few of chillers are engaged. The space between chiller outlets and inlets is the domain where the mixing of the warm and cold coolant occurs. For instance, figure 5 represents the case when chiller 1 and chiller 4_5 are used only. The length of the divider is 6250 mm and its diameter equals 400 mm. Diameters of pumps and chillers inlets and outlets are 250 mm and 125 mm respectively. The volume of the collector equals 853 623 cm^3.

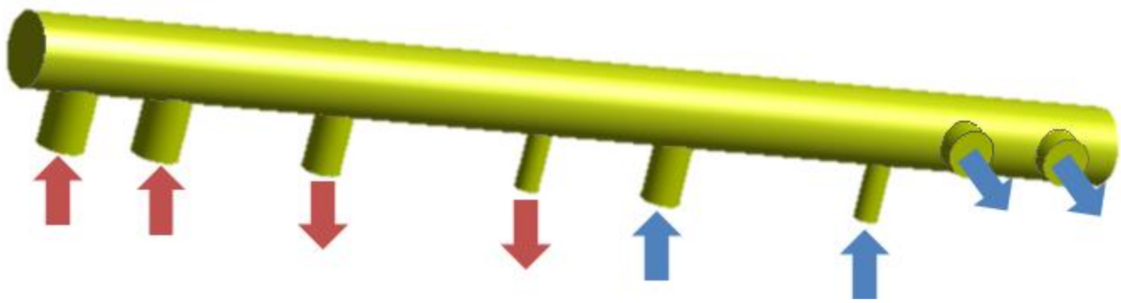

Fig. 5. Outline of the 3D fluid divider when chiller 1 and chiller 4_5 are used only.

3.2 Mesh

In order to create the mesh, cut cell approach was chosen. This method [1] uses an uniform stationary background Cartesian mesh. The background mesh is constructed first and solid regions are subsequently cut out of it. Cut cells which have one of their sides coincident with boundary segment are defined by the boundary intersections. As a result a boundary conforming mesh is generated, without the necessity to make the boundary a coordinate surface. The only important issue in this method is to calculate the intersections of a series of line segments with the background Cartesian mesh. In simplified circular geometry and coarse mesh result of the cut cell method is shown in Fig 6:

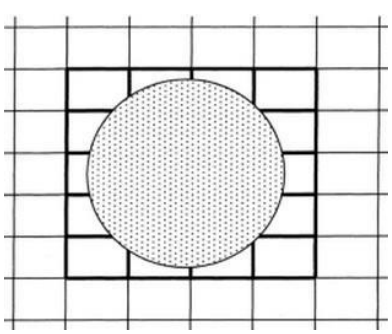

Fig. 6. An example of the cut cell method on simplified geometry [2].

Moreover, it is worth to point out other cut cell mesh advantages [3]:

- It is always body-fitted;
- It provides simultaneously high fidelity geometric representation and a very coarse mesh;
- It has better mesh quality parameters than other approaches, i.e. lack of skewness;
- It assumes cell refinement at the wall.

In order to model appropriately velocity profiles near the wall of the flow domain, especially at the inlet sections, it was necessary to apply set of boundary layers. In order to improve the model of the steady state, the simulation of the inlet flow was conducted, assuming periodic boundary conditions on an inlet pipe. The stable fluid flow profile has been formed after certain number of flow cycles. The results of different number of boundary layers showed that adding more than 6 boundary layers had no visible impact on the shape of velocity profiles under assumed coolant load. Hence, it was decided that 6 layers model is appropriate for this kind of issues.

Subsequently, the divider geometry was cut by the mesh grid (fig. 7 and 8). Its detailed description can be found in Table 1.

Table 1. Mesh parameters.

Mesh parameter	**Value**	
Number of nodes	745 889	
Number/type of elements	Hexahedrons:	705739
	Wedges:	22974
	Tetrahedrons:	146
	Pyramids:	98
	TOTAL:	728957
Mesh type/-s in use	CutCell	
Volume	Minimum cell volume :	0.0311 cm^3
	Maximum cell volume (m3):	3.3181 cm^3
	Domain volume:	853 623 cm^3

Mesh quality	Skewness > 0.95: 16 elements Orthogonal quality < 0.15: 0 elements
Boundary layer	Method: smooth transition Number of layers: 6 Growth rate: 1.2 Transition ratio 0.272

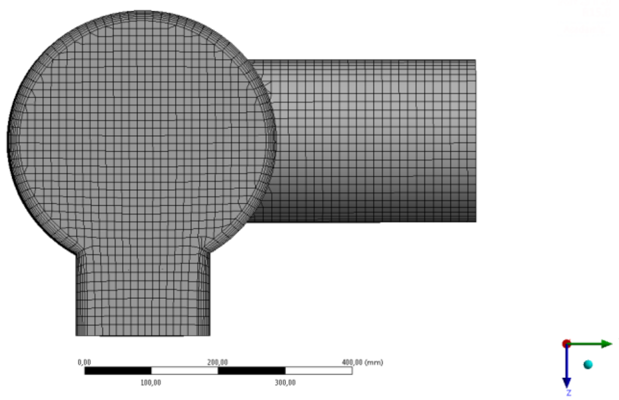

Fig. 7. A y-z cross-section.

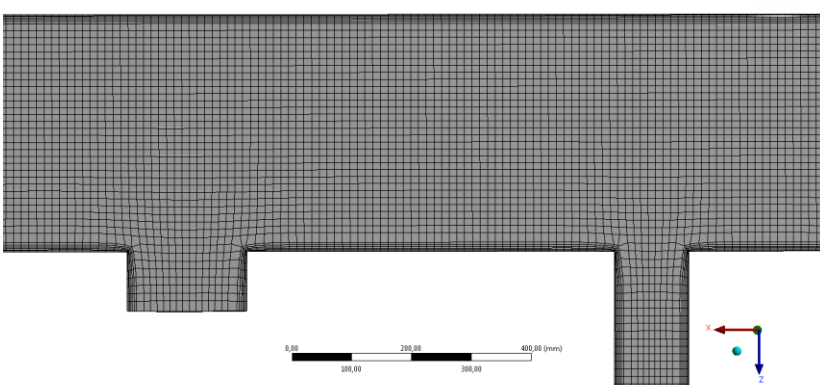

Fig. 8. A x-z cross-section through the mesh.

Approximately 728 thousands cells, six boundary layers on every wall of the divider and good mesh parameters might be a premise that the results of the simulation will coincide with the real operating conditions. It is possible to improve this values, but it could make this system too robust, making the simulation of the transient state impossible in limited amount of time. Hence, the generated mesh was accepted to be adequate for this kind of problem.

3.3 CFD Setup

Knowing that the cooling power is coupled with the server electric power loads, it is rational to assume that the fluid divider will be always in a transient state. However, to perform a simulation, some boundary conditions, with the assumed fluid flow, are needed. As it was mentioned before, the divider is treated as a black box, so it is impossible to measure real coolant loads and apply them to inlets. Additionally, to start the transient simulation from the reasonable point, when the temperature fronts are set, steady state pre-simulation is needed. Summarizing, several different work regimes with different fluid flow loads are needed to be investigated, both for transient and steady state. Limiting the number of variants to feasible amount, 5 load variants were chosen for further investigation:

- **Variant I**
  40 l/s load with 2 pump and 2 chillers working (pump_A, pump_B, chiller_1, chiller_4_5)
- **Variant II**
  40 l/s load with 1 pump and 2 chillers working (pump_A, chiller_1, chiller_4_5)
- **Variant III**
  20 l/s load with 1 pump and 2 chillers working (pump_A, chiller_1, chiller_4_5)
- **Variant IV**
  20 l/s load with 1 pump and 1 chillers working (pump_A, chiller_4_5)
- **Variant V**
  80 l/s load with 1 pump and 3 chillers working (pump_A, chiller_1, chille_3 chiller_4_5)

All of them are presented in figure 9:

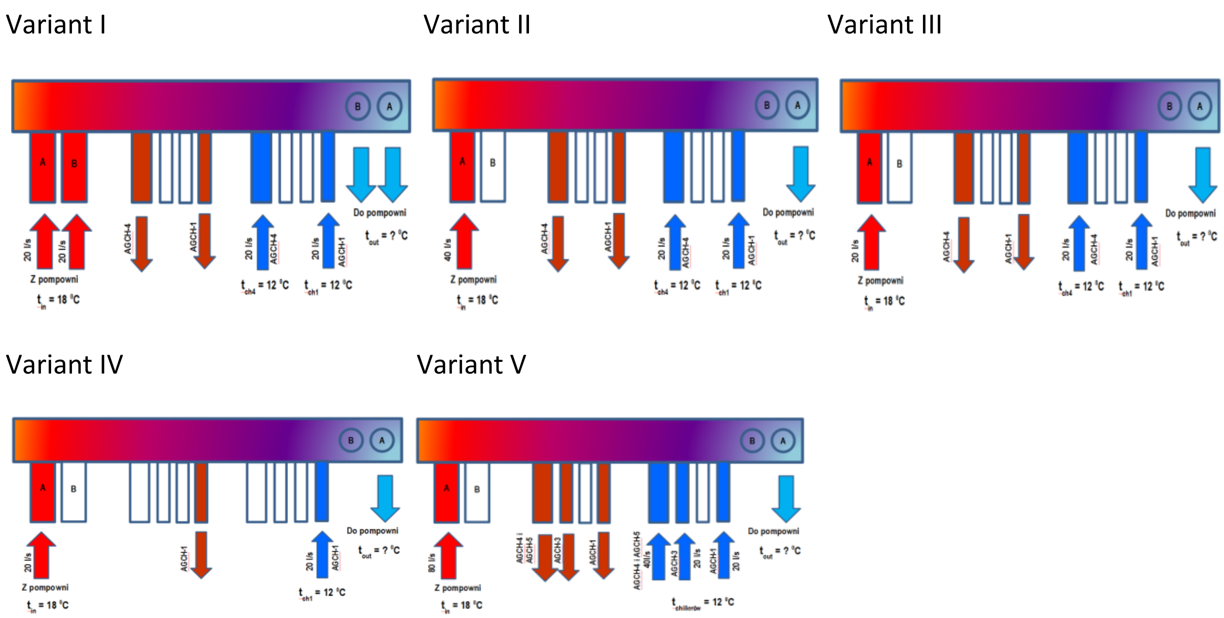

Fig. 9 Variants of the coolant loads.

One comment here is necessary. The best practice in CFD is to build a fine mesh suitable to the pre-assumed initial conditions in the specific model, however it is also reasonable to build the generic mesh of the resolution that will catch the effects of turbulence in the most complicated case and this one will be a reference for further studies. Such an approach was applied in the following study.

While referring to a turbulence, it has to be mentioned that k-kl-ω model was used in all presented simulations (transient and steady state). This model was chosen from among other Reynolds Averaged Navier Stokes (RANS) formulations basing on sensitivity study, which is not a matter of discussion here. The k-kl-ω model was used mostly due to its capability of predicting laminar-to-turbulent flow developments [6].

The k-kl-ω model governs three additional transport equations which are solved by the program. First equation (Eq. 1) defines turbulent kinetic energy (k_T), the second (Eq. 2) describes the laminar energy (k_L) and the third (Eq. 3) corresponds to the scale-determining variable (ω), defined as $\omega=\varepsilon/k_T$, where ε is the isotropic dissipation. The transport equations are as follows:

$$\frac{Dk_T}{Dt} = P_{k_T} + R_{BP} + \omega k_T - D_T + \frac{\partial}{\partial x_j}\left[\left(\nu + \frac{\alpha_T}{\sigma_k}\right)\frac{\partial k_T}{\partial x_j}\right] \qquad (1)$$

$$\frac{Dk_L}{Dt} = P_{k_L} + R_{BP} - D_T + \frac{\partial}{\partial x_j}\left[\nu \frac{\partial k_L}{\partial x_j}\right] \qquad (2)$$

$$\frac{D\omega}{Dt} = C_{\omega 1}\frac{\omega}{k_T}P_{k_T} + \left(\frac{C_{\omega R}}{f_W} - 1\right)\frac{\omega}{k_T}(R_{BP} + R_{NAT}) - C_{\omega 2}\omega^2 + C_{\omega 3} f_\omega \alpha_T f_W^2 \frac{\sqrt{k_T}}{d^3} + \frac{\partial}{\partial x_j}\left[\left(\nu + \frac{\alpha_T}{\sigma_\omega}\right)\frac{\partial \omega}{\partial x_j}\right] \quad (3)$$

The various terms in the model equations represent production, destruction, and transport mechanisms. It is important to mention that the model uses inverse turbulent-time scale (ω) rather than the dissipation rate (ε) like k-ε model does.

Furthermore, the investigation of the turbulence model was performed. Four chosen models were considered (see fig. 10 to 13).

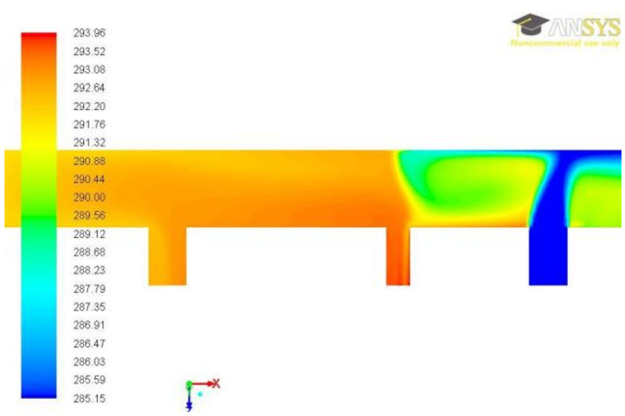

Fig. 10. Static temperature, k-kl-ω in variant III (40l/s).

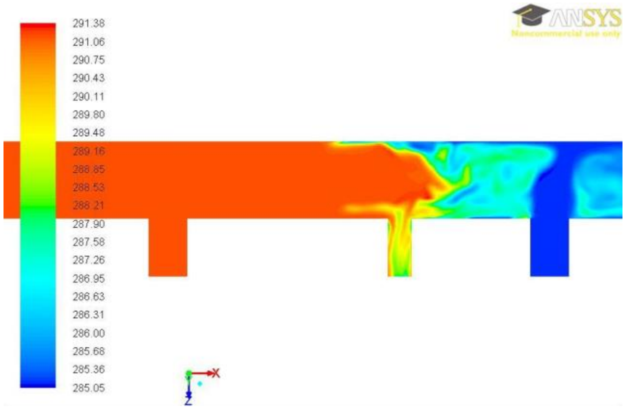

Fig. 11. Static temperature, laminar model in variant III (40l/s).

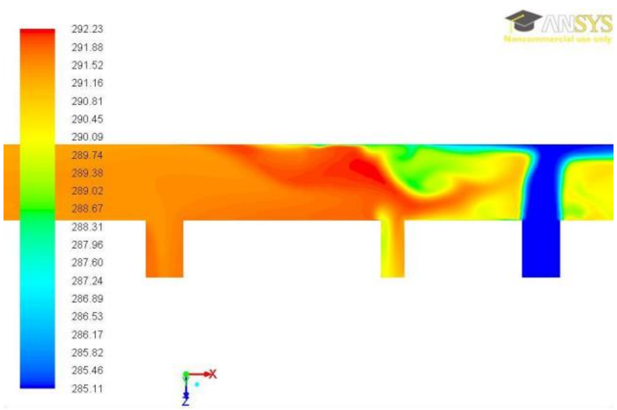

Fig. 12. Static temperature, k-ω in variant III (40l/s).

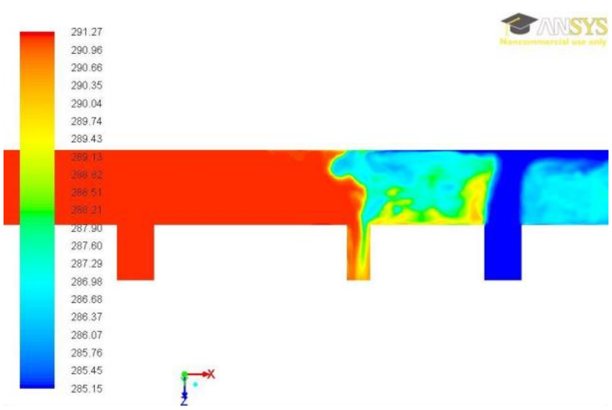

Fig. 13. Static temperature, LES in variant III (40l/s).

The LES turbulence model provides the most accurate solutions [7], however, it is the most computationally demanding model as well. The number of the grid cells, required to create appropriate mesh for the LES, is too big to simulate this problem in a reasonable amount of time, especially in transient state. The k-kl-ω is the example of the RANS model that averages the LES solution (for static temperature) better than the other considered RANS models (laminar, k-ω, k-ε) and provides satisfactory accuracy of the results. Furthermore, residuals plots (see fig. 14 to 17) eliminate the possibility of the laminar model use, indicating to high values of the residuals there.

Considering all provided above arguments, the k-kl-ω was chosen because of the lowest residuals, acceptable computation time and more satisfactory approximation of the LES solution than in the case of the k-ω.

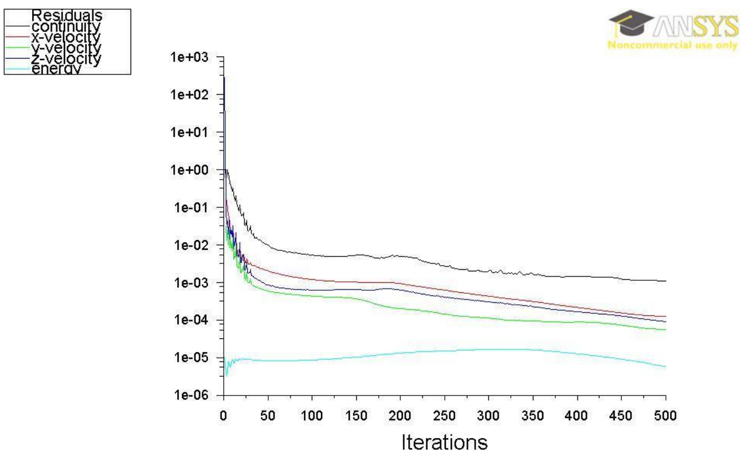

Fig. 14. Residuals k-kl-ω.

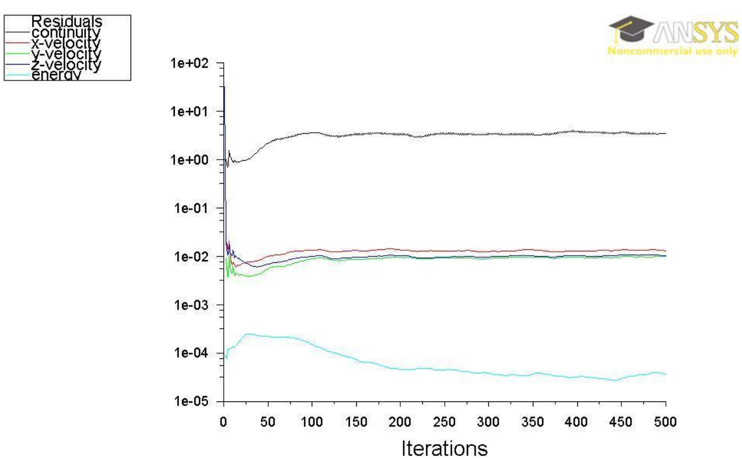

Fig. 15. Residuals laminar model.

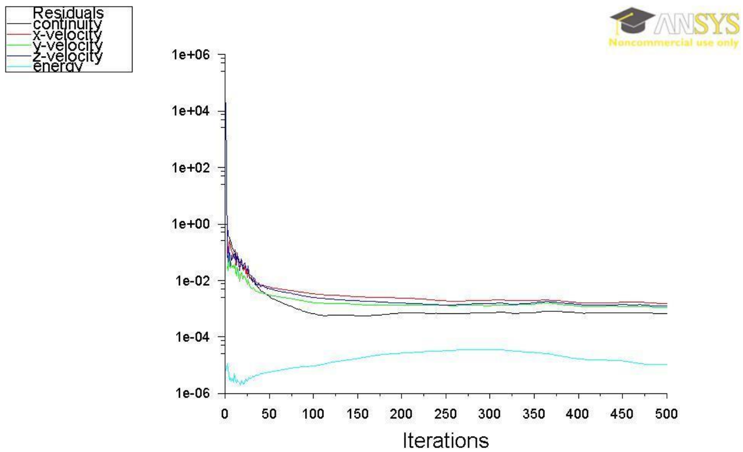

Fig. 16. Residuals k-ω.

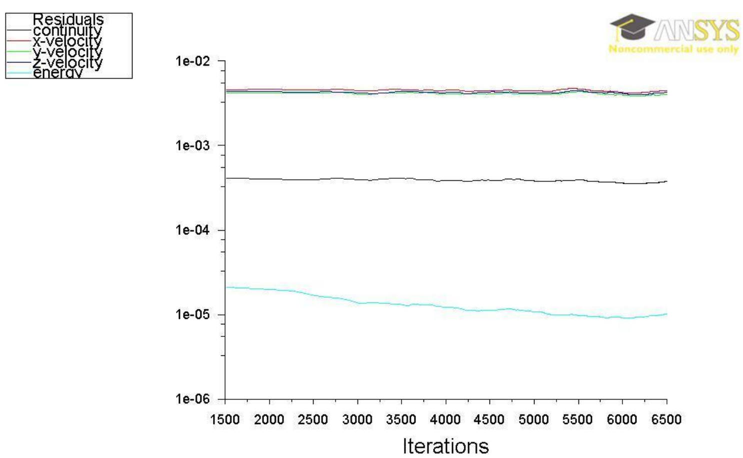

Fig. 17. Residuals LES.

As it is presented in fig. 18, the turbulent Reynolds number varies from 2 to almost 60000. This is the reason why it is reasonable to concentrate on predicting laminar-to-turbulent transition more accurately. The initial and boundary conditions used for hydraulic divider simulation in variant III (representative variant) are shown in table 2. Hydraulic load may vary in other variants, but the rest of conditions remain the same.

Thanks to its features, this model should relatively easy catch different turbulent mechanisms, i.e. turbulence due to sudden change in flow direction or due to mixing in a counter-flow.

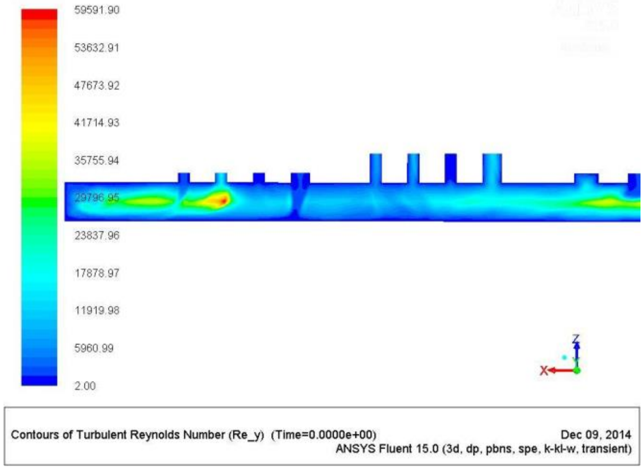

Fig. 18. Reynolds number in variant V (80l/s).

Table 2. Boundary and initial conditions in variant III.

Condition	Definition	Fluid load	Temperature
Inlets (pre-calculated velocity profiles were applied)	Pump A	20 l/s	291.15 K
	Pump B	20 l/s	291.15 K
	Chiller 1	20 l/s	285.15 K
	Chiller 2	0	-
	Chiller 3	0	-
	Chiller 4_5	20 l/s	285.15 K
Outlet	Outflow - proportional to inlet values		
Wall	Stationary wall with no slip condition		
Gravity	9.81 m/s^2 (z-axis)		

Investigated domain contains only a fluid part. No mechanical stresses nor heat transfer to or from the external environment are evaluated, so there is no need to take into account a solid part of the fluid divider. Therefore, only one cooling medium will be taken under the consideration - namely glycol. Its material properties are presented in Table 3.

Table 3. Properties of coolant: 38% ethylene glycol solution.

Property	**Value**	**Unit**
Density	1054	kg/m^3
Specific heat	3550	J/(m*K)
Thermal conductivity	0.43	W/(m*K)
Viscosity (piecewise linear)	0.00796824 (263.15K) 0.00382602 (283.15K) 0.0027931 (293.15K) 0.00135966 (323.15K)	kg/(m*s)

Next part of CFD setup is a solver selections. In this case SIMPLE (Semi-Implicit Method for Pressure-Linked Equations) solver was chosen. The algorithm proceeds as follows [5]:

1. An approximation of the velocity field is obtained by solving the momentum equation. The pressure gradient term is calculated using the pressure distribution from the previous iteration or an initial guess.
2. The pressure equation is formulated and solved in order to obtain the new pressure distribution.
3. Velocities are corrected and a new set of conservative fluxes is calculated.

Special discretization schemes that were selected are listed in table 4.

Table 4. Spatial discretization.

Variable	Discretization method
Gradient	Green-Gauss Cell Based
Pressure	Standard
Momentum	Second Order Upwind
Turbulent Kinetic Energy	Second Order Upwind
Laminar Kinetic Energy	Second Order Upwind
Specific Dissipation Rate	Second Order Upwind
Species Concentration	Second Order Upwind
Energy	Second Order Upwind

Transient simulations were conducted assuming the time step equals 0.00034 s and 20 s of total simulation time.

3.4 Results

Applying all the methods pointed above and conditions for transient and steady states, various data were obtained. In order to find the reasons of instabilities inside the divider, two the most important parameters were selected to the final comparison, namely:

- Temperature distribution,
- Glycol concentration (mass fraction) at domain outlets with respect to the flow origin.

Temperature distribution in steady state simulation, presented in figures 19 to 23 did not indicate any clear temperature front, that shows a stationary mixing zone in the fluid.

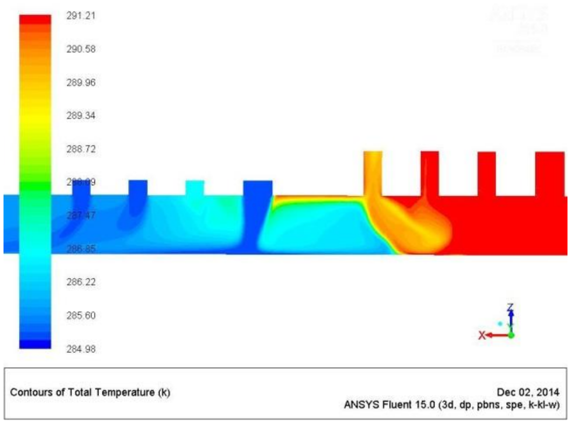

Fig. 19. Temperature Variant I (40l/s).

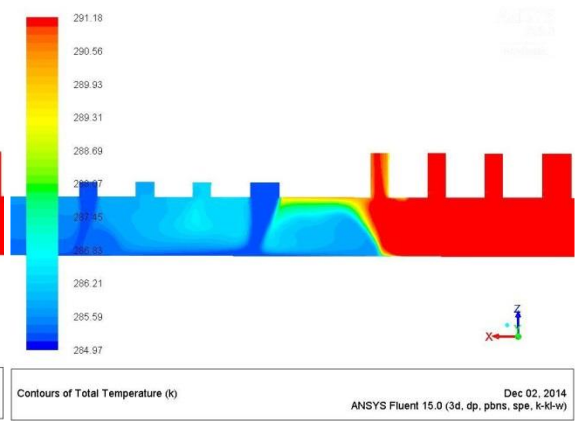

Fig. 20. Temperature Variant II (40l/s).

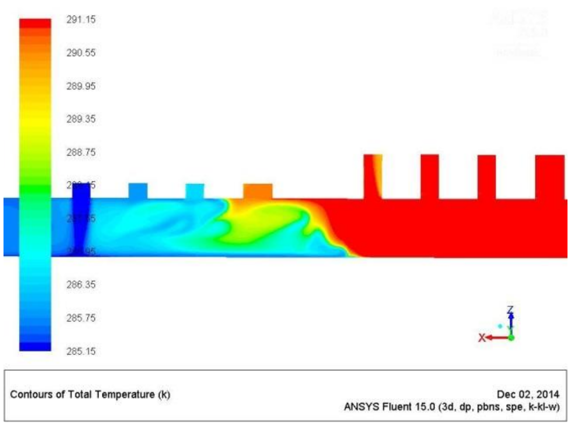

Fig. 21. Temperature Variant III (20l/s).

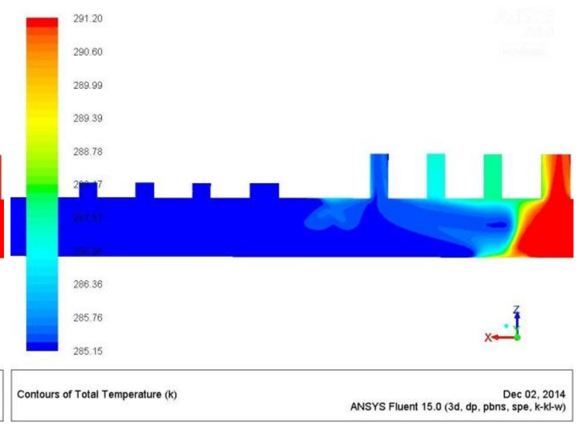

Fig. 22. Temperature Variant IV (20l/s).

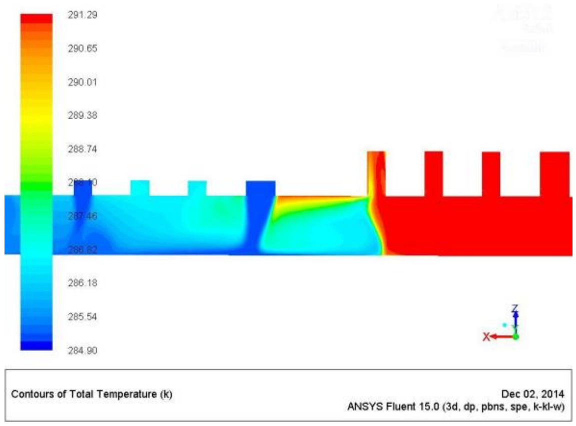

Fig. 23. Temperature Variant V (80l/s).

The proof of instabilities in transient state can be found in figure 24, where temperature contours from every two seconds of Variant V simulation (11 frames) are shown. This can be the proof why the highest residuals (continuity equation) reached the high level of 2 * 10^{-2} after 2000 iterations in steady state simulation. In the transient, these residuals were 3 orders of magnitude better (1 * 10^{-5}). Considering these results, one may conclude, that turbulent and time-dependent character of the flow cannot be recreated in the steady state simulation, so only transient state may show the variety of the states satisfying the transport equations and the boundary conditions.

t = 0 t = 2 sec t = 4 sec

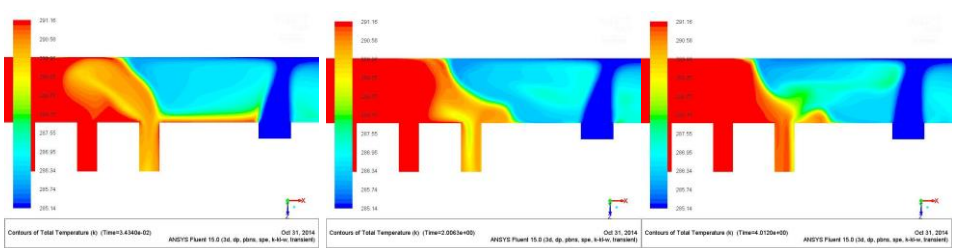

t = 6 sec t = 8 sec t = 10 sec

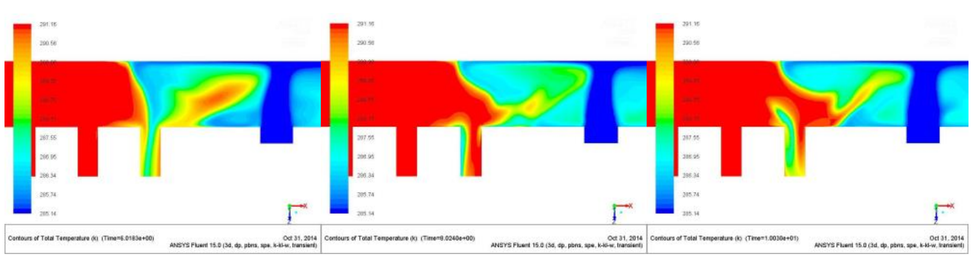

t = 12 sec t = 14 sec t = 16 sec

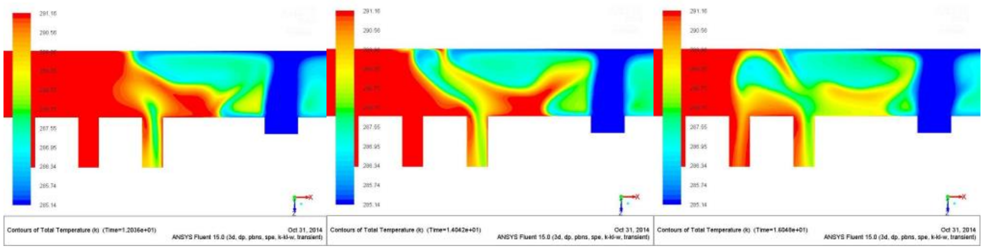

t = 18 sec t = 20 sec

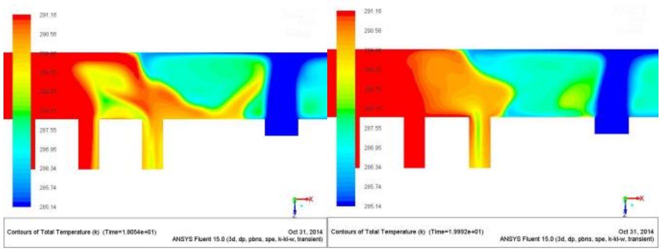

Fig. 24. Total temperature in transient Variant V.

Transient results of variant V simulation (coolant load = 80 l/s) clearly show that the temperature oscillations in the fluid mixing zone (central part of the container) are significant and easily observable. In order to investigate this more accurately, plots of the average temperature and mass fraction of coolants with respect to the origin of a source were created. Mass fractions and temperatures in all variants are presented on Fig 25:

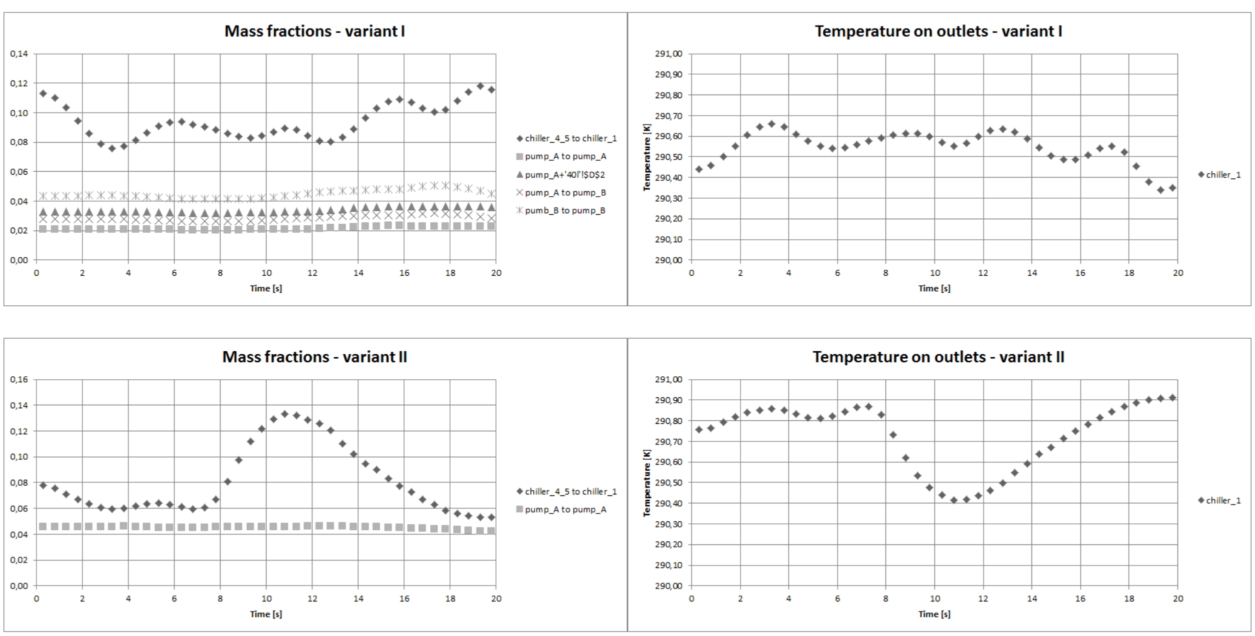

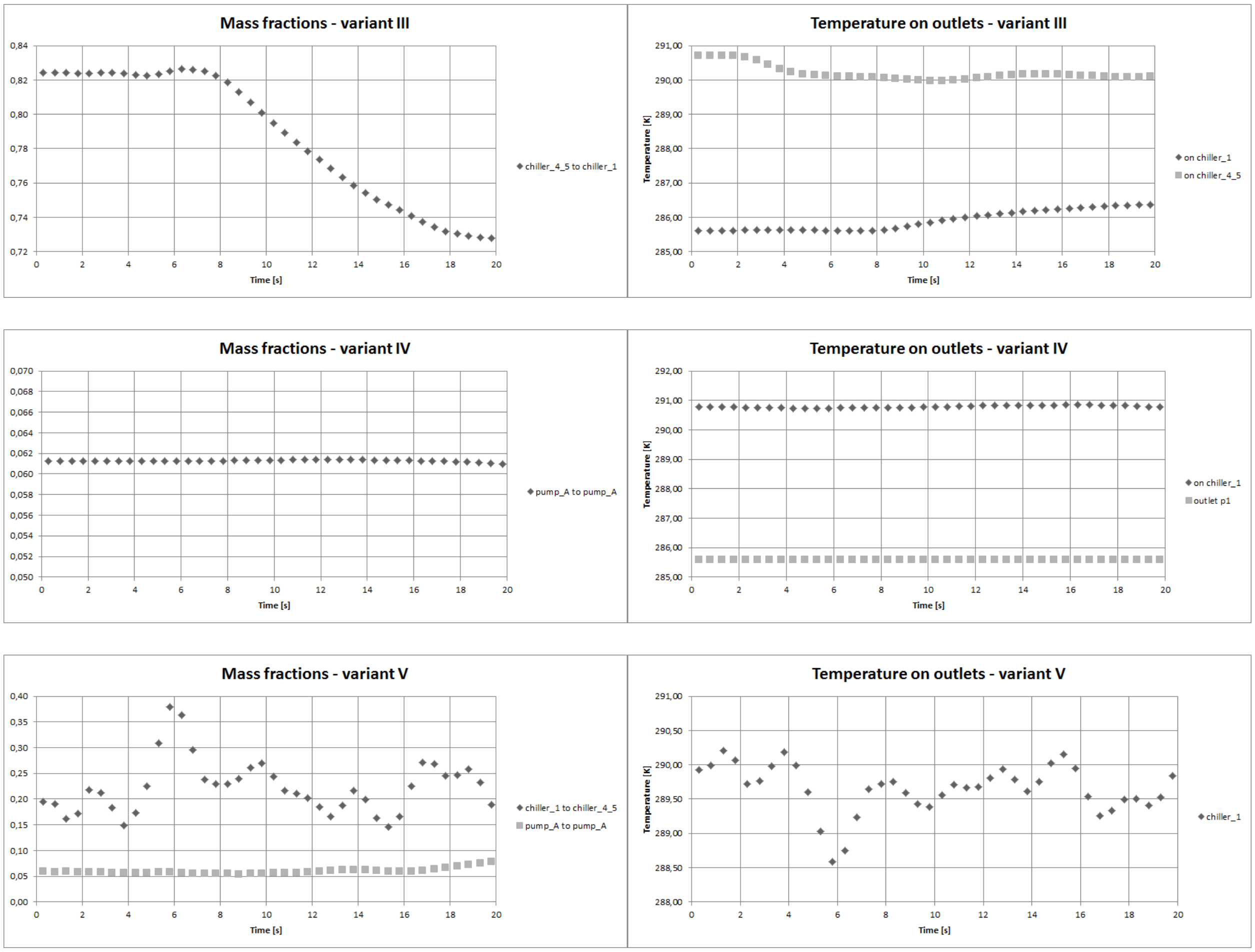

Fig. 25. Average temperature and mass fraction on fluid divider outlets.

At the first glance, only IV seems to work stable. The temperature oscillations in the least stable Variant (80 l/s) has an amplitude of 1.5 K which means 25% of maximum temperature gradient in the container. It might have negative influence on the cooling control system. As an impact of that, chillers may switch on and off alternately even if the cooling demand is remaining constant, causing inefficient use of them and higher energy consumption. The mass fraction plots may prove this unstable work. In some cases (Variant V) coolant concentration from chiller 1 on chiller 4_5 varies between 15% to 35% in respect to the whole fluid flux coming from chiller 1 . The fluid flow also has considerable impact. Higher cooling load causes more dynamic mixing process and stronger oscillations. In every case, there was no element that could stabilize the temperature front. Thus, in all simulations of the current fluid divider transient, mixing zones were constantly changing their positions in the fluid divider.

4. New geometry application

Since the current geometry of the fluid divider is suspected to be the cause of instabilities of fluid flow, new modifications of the geometry must be considered. The most likely space for oscillations occurrence is situated in the domain between inlets and outlets to the chillers. This is the place where cold and hot stream are mixing during the transient (presented on the fig. 26) .

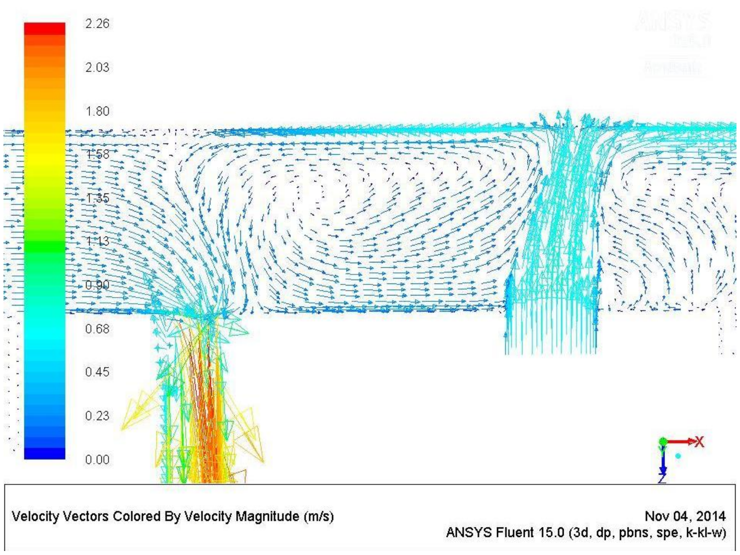

Fig. 26. Velocity magnitude in the mixing zone.

It is easily seen that the stream from cold chiller leg (stream from the right pipe) strikes directly into the upper wall of the collector and the part of it is directed to the hot chiller leg (stream to the left pipe). From the cooling point of view it would be favourable (stage cooling improves COP), but here unstable mixing at fluid, with strong oscillations is observed. Furthermore, the part of the flow omits the chillers and goes directly from the pump outlet to the pump inlet and it has to be fixed as well. Hence, several geometry modifications of the fluid divider central part were examined. The best way to present variety of geometries investigated in this project is presenting them on a map cases (shown in the table 4). Various modifications and load variants were taken into account in this project in order to find the most efficient one. As a result of that, two modifications with the most stable fluid flow were selected based on the obtained results: sieve baffle and narrowing. Furthermore, applied baffles had the same cross-section area of the fluid flow, equivalent the area of circle with the diameter of 152 mm. Diameter of the holes in a sieve baffle was assumed to be equal to 10mm, in order to simplify the manufacturing process.

At the beginning of the project, an idea of extending the central part of the divider by one meter appeared. It might lead to close the mixing zone in the extended domain between chiller inlets and outlets and weaken any sort of instabilities there. However, extension could not be longer than 1 m due to the necessity of placing it on the roof with limited dimensions.

Table 4. Examined cases and geometries.

Name	**Geometry**	**Cases**
No modification		● 20 l/s (steady) ● 20 l/s (transient) ● 40 l/s (steady) ● 40 l/s (transient) ● 80 l/s (steady) ● 80 l/s (transient)
Extended	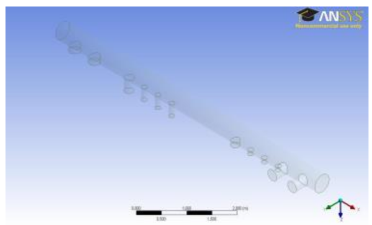	● 20 l/s (steady) ● 20 l/s (transient) ● 40 l/s (steady) ● 40 l/s (transient) ● 80 l/s (steady) ● 80 l/s (transient)
Sloping baffles (both for upper and lower baffles)	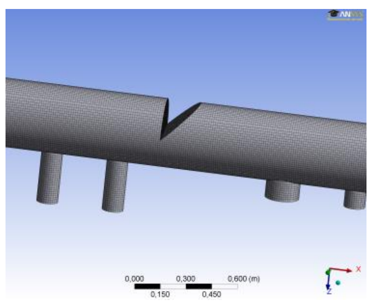	❑ Closer baffle ● 20 l/s (steady) ● 40 l/s (steady) ● 40 l/s (transient) ● 80 l/s (steady) ❑ Central baffle ● 20 l/s (steady) ● 40 l/s (steady) ● 40 l/s (transient) ● 80 l/s (steady) ❑ Further baffle ● 20 l/s (steady) ● 40 l/s (steady) ● 40 l/s (transient) ● 80 l/s (steady)

Flat baffles (both for upper and lower baffles)	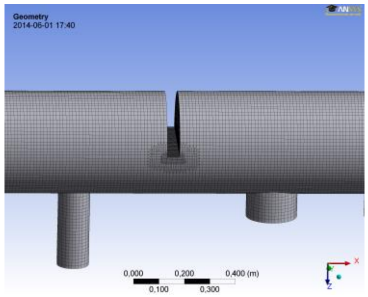	• 20 l/s (steady) • 40 l/s (steady) • 40 l/s (transient) • 80 l/s (steady)
Sieve	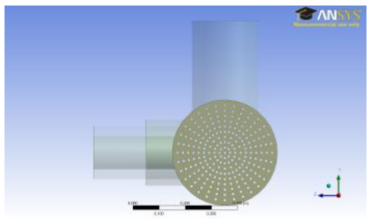	• 20 l/s (steady) • 20 l/s (transient) • 40 l/s (steady) • 40 l/s (transient) • 80 l/s (steady) • 80 l/s (transient)
Narrowing	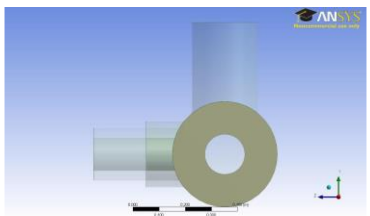	• 20 l/s (steady) • 20 l/s (transient) • 40 l/s (steady) • 40 l/s (transient) • 80 l/s (steady) • 80 l/s (transient)

5. Results comparison

In this comparison of chosen cases, a few key parameters were analysed in order to find the best geometry modification, giving the most stable fluid flow predictions:

- mass fraction of coolant at outlets,
- temperature at outlets.

5.1 System load I (40 l/s)

It is a case where both pumps and two chillers were working. The results are plotted below:

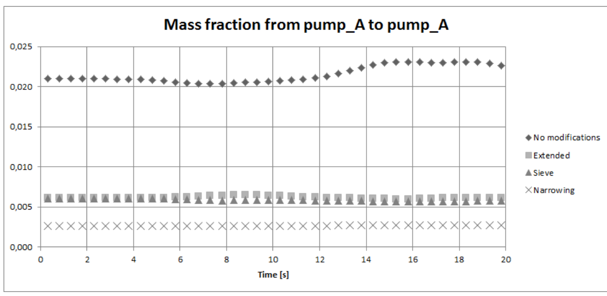

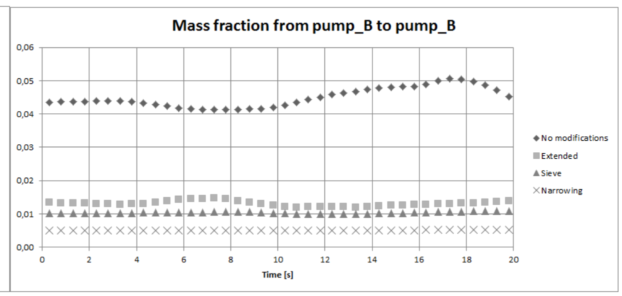

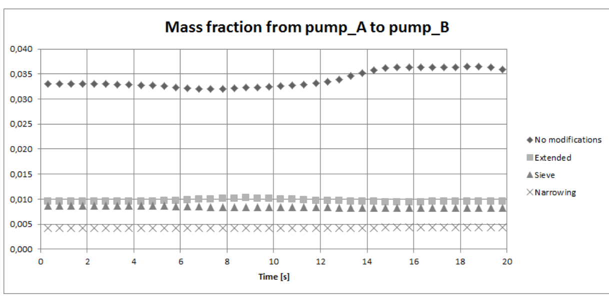

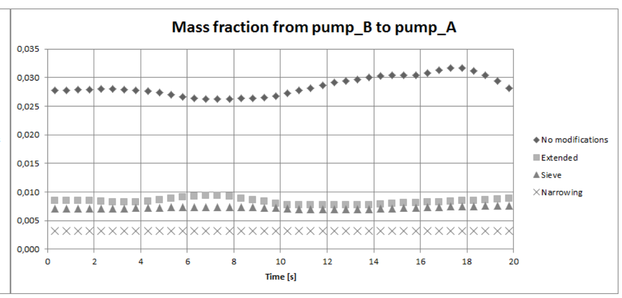

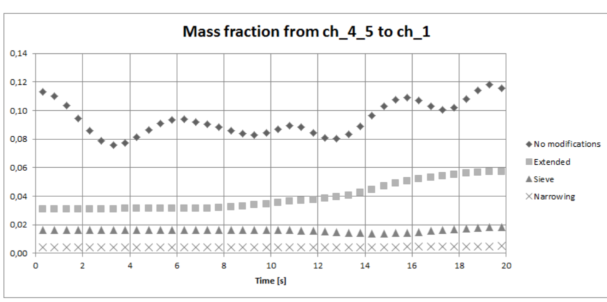

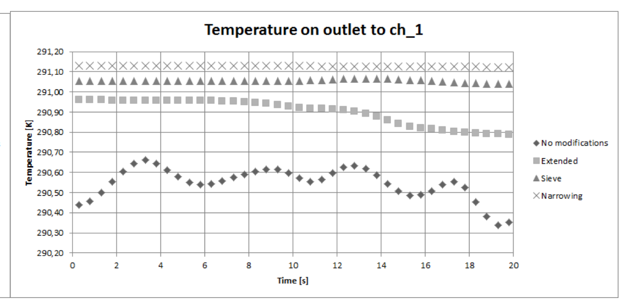

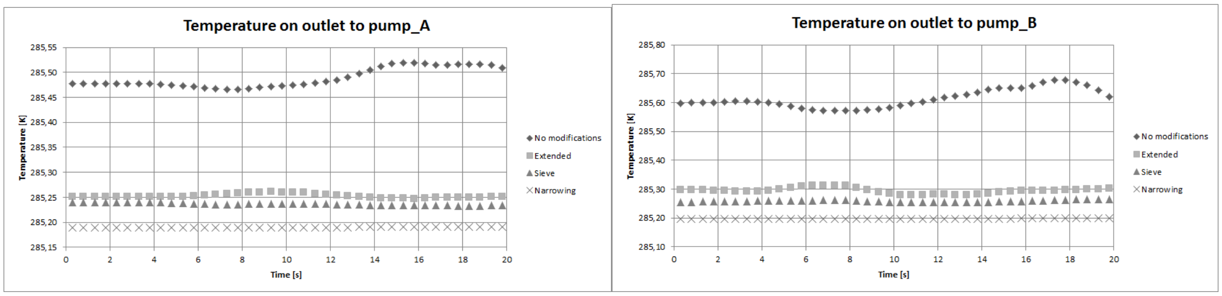

Fig. 27. Temperatures and mass fractions in Variant I.

Beginning from the reference case (with no modifications), it is worth to highlight how much coolant is by-passing the chiller system. Summing the mass fractions from pump A to B and A to A gives approximately 5.5 % of the stream from the pump A omitting the chillers. Similar result can be obtained in case of the pump B, where 7.5 % of the fluid is not cooled by the chillers. Changing the geometry of the divider, allows to decrease these values to 2.5% (extended divider) or even 0.75% (with use of narrowing baffle) what will result in decrease in temperature on outputs to pumps. Thus, the cooling of the server room would be improved.

Next challenging issue is the oscillations' appearance that can be observable both in the mass fractions and the temperatures on the inlet to chiller 1. Reference scenario (no modifications) illustrates a significant instabilities in the fluid flow in the mixing part of the divider. Changes of the mass fraction of the coolant flowing from the chiller 4 to chiller 1 are equal more or less to 4 % which means ⅓ of the coolant transported in this way (4% from 12% max). It is crucial considering automatic systems that controls the cooling during the constant cooling demand. Basing on the plotted values, the use of a baffle (either with sieve or narrowing) can stop this effect totally. Even the case with extension shows that some precipitation of balance occurs after 10th second. On the other hand main disadvantage of using the baffles is a limitation of stage cooling and coolant flow between chiller 4 and chiller 1.

5.2 System load II (40 l/s)

In this hydraulic load system, one pump and two chillers were working.

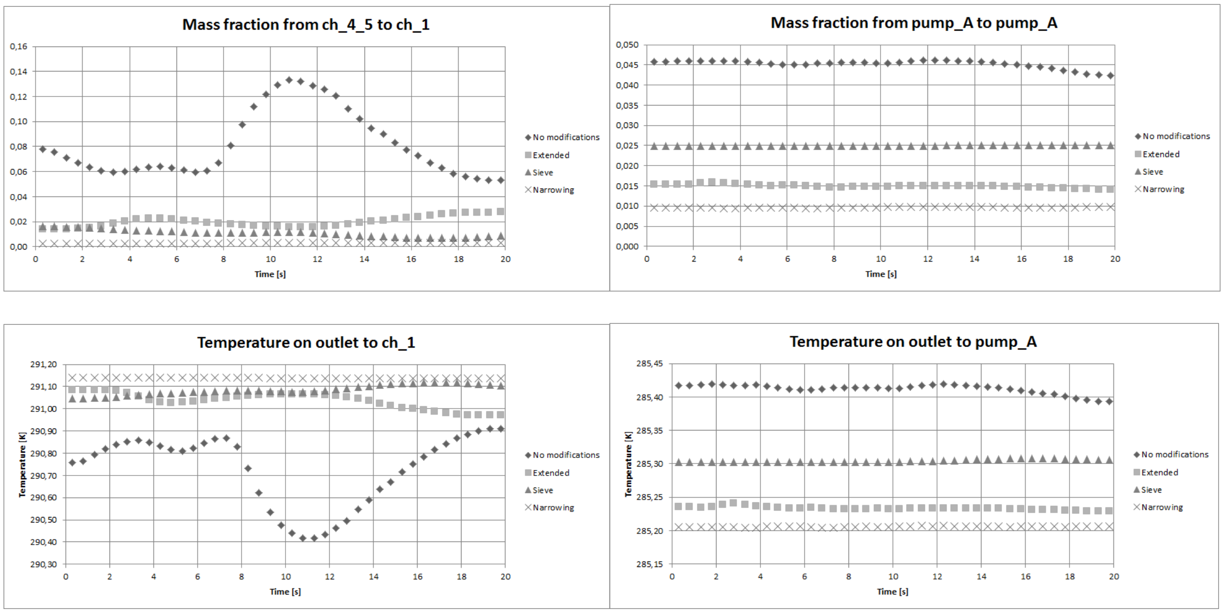

Fig. 28. Temperatures and mass fractions in variant II.

In this fluid load variant, the current divider (no modifications) works inefficient as well, mostly because of the by-passing the chiller system by the part of the coolant (4.5% of the total mass) and temperature fluctuation appearance. On the outlet to chiller 1 the amplitude of the temperature reaches 0.5K what is 8.3% of the total temperature gradient in the container. Each of the proposed geometry might be perceived as a sort of solution to the occurring instabilities. However, the narrowing baffle seems to give the best results, mostly considering the significant limitation of the coolant by-passing (below 1%) and the lowest temperature on outlet to pump A.

5.3 System load III (20 l/s)

In this case, one pump and two chillers were turned on.

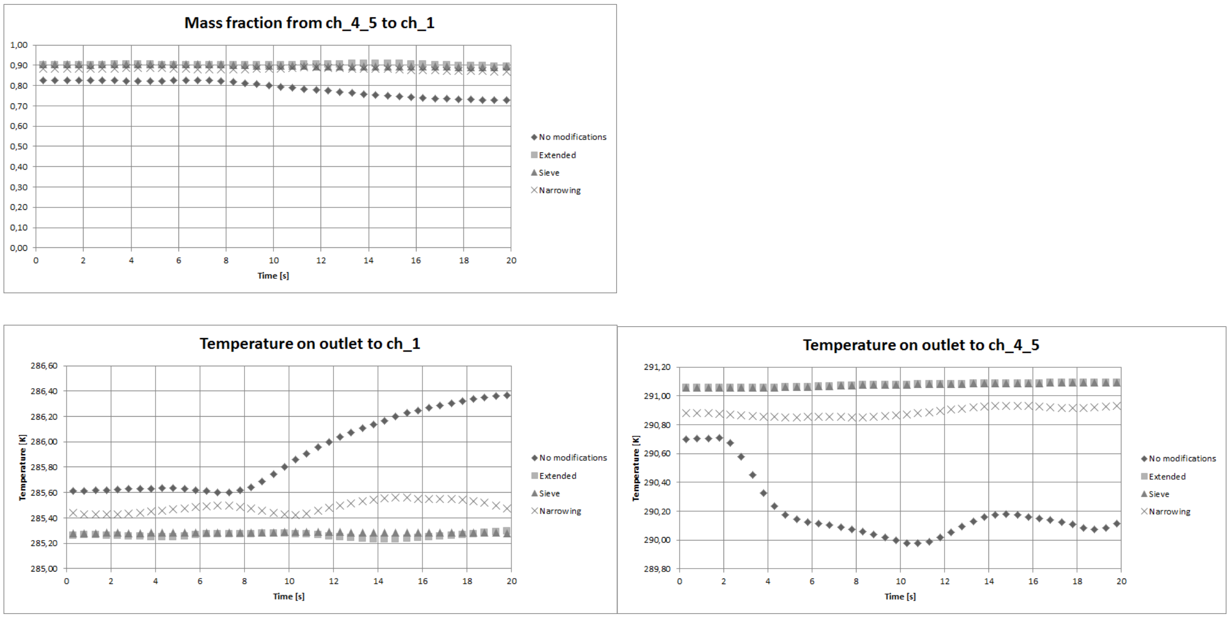

Fig. 29. Temperatures and mass fractions in variant III.

The system load here is the lowest from all considered variants. Plots above show that all 3 geometry modifications might be applied in order to cope with instabilities of the coolant flow. The case with a narrowing baffle is slightly less stable than other 2 modifications, but on the other hand this type of baffle improves the efficiency of the cooling process in chillers by decreasing the temperature on chiller 4 inlet (increase of COP) and rising the coolant temperature on the outlet to chiller 1 (better coolant mixing). The temperature oscillations in divider with narrowing are insignificant for chillers' controllers due to the too small magnitude (less than 0.15 K). It is worth to mention that in this less loaded case reference case shows changes of the temperature about 0.8 K what can be substantial, considering total change of the coolant temperature on chillers equals 6 K.

5.4 System load IV (20 l/s)

In this hydraulic load system, one pump and one chiller were considered.

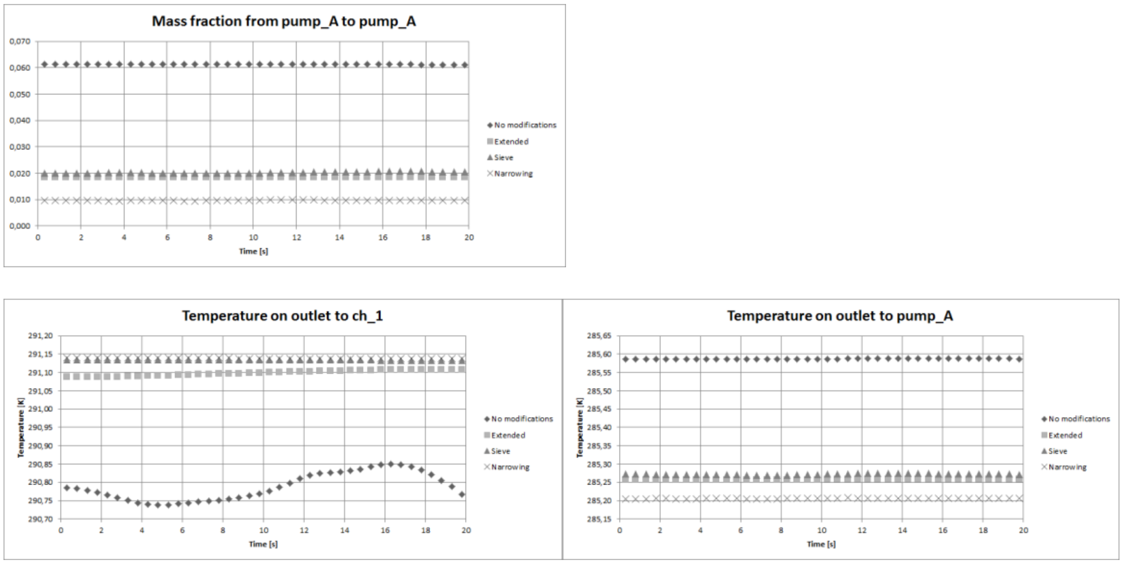

Fig. 30. Temperatures and mass fractions in variant IV.

This is the most stable case, even for the current divider, what is easily visible in mass fraction and temperature on outlet to pump A plots. The only issue to comment is by-passing problem. In the “no modification” case it is a 6% of the total mass omitting the chillers. Although every considered modification solves the problem: mass fraction omitting chillers limited either to 2% (extended geometry, sieve baffle) or 1% (narrowing baffle).

5.5 System load V (80 l/s)

In this last case, one pump and three chillers were assumed to be turned on.

Cooling load equals 80 l/s and due to this, it is the most dynamic case. Simulation results are plotted in figure 31. Current divider simulation shows that the work of the divider is unacceptable, because of the significant temperature gradient (1.5K) and fluctuations of the mass fraction on outlet to chiller 1 that varies from 15% to 40%. Plots show that all geometry modifications might be treated as a solution, but only the case with the narrowing provides the lowest temperature on outlets to pumps and the most stable coolant flow, as it was in other variants.

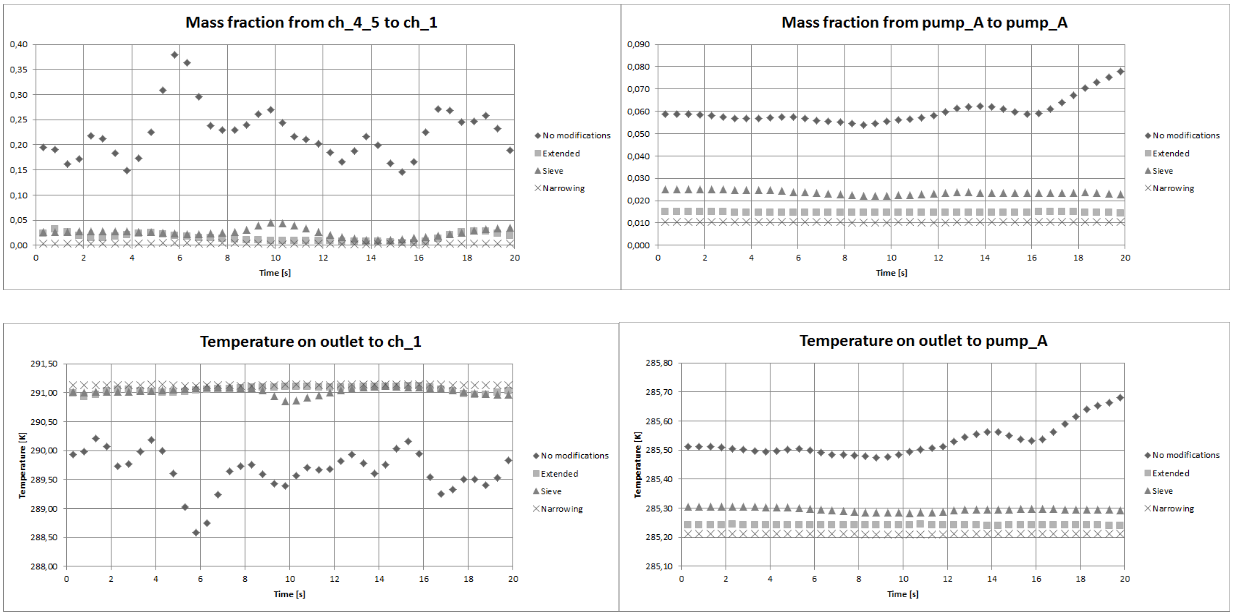

Fig. 31. Temperatures and mass fractions in variant V.

6. Conclusions

Application of the CFD analysis allows us to simulate the coolant flow in the domain where it was impossible to install any measurements devices. As an impact of that, the reasons of occurring anomalies were indicated. Summarizing the results of simulations and taking into account various number of cases, the following conclusions can be made:

- Current fluid divider simulation indicated two problems occurring in its work: fluctuation in mass fractions on chiller outlets and by-passing the chiller system by the part of the coolant. Both of them have negative effect on chillers' efficiency.

- The domain between chiller inlets and outlets is the space where mixing occurs and temperature gradient is the highest.

- Higher fluid load causes stronger fluctuations especially in "no modification" case.

- To support the temperature front and to make it stationary, a baffle in the central domain is needed.

- Steady state simulation was not enough to select the most optimal geometry, transient is necessary in this kind of problems.

- Narrowing and sieve baffle cope the best with instabilities in the fluid. Extended geometry sometimes does not provide a solution (i.e. Variant I - mass fraction on inlet 1 plot).

- Narrowing baffle case provides always the lowest temperature on outlets to pumps.

- Differences between narrowing and sieve baffle were relatively small, but the geometry of narrowing is much simpler to manufacture so the narrowing is the modification that is recommended to apply.

7. Acknowledgements

All the simulations that became a basis for this paper were conducted thanks to the EU and MSHE grant no. POIG.02.03.00-00-013/09 - Świerk Computing Centre (www.cis.gov.pl).

8. References

[1] D.M. Causon, D.M. Ingram, C.G. Mingham "A Cartesian cut cell method for shallow water flows with moving boundaries" Centre for Mathematical Modelling and Flow Analysis, Manchester Metropolitan University, Manchester February 2001.

[2] P.G. Tucker, Z. Pan "A Cartesian cut cell method for incompressible viscous flow" Fluid Dynamics Research Centre, School of Engineering, The University of Warwick, December 1999.

[3] R.Kaczmarek, "It's All about The Mesh – A Cartesian Cut-Cell Approach" http://www.convergecfd.com/its-all-about-the-mesh-cartesian-cut-cell-approach/#sthash.mAkY5aZd.dpuf, August 19, 2013.

[4] H. Rahimi, W. Medjroubi, J. Peinke, "2D and 3D Numerical Investigation of the Laminar and Turbulent Flow Over Different Airfoils Using OpenFOAM" First Symposium on OpenFOAM in Wind Energy, Oldenburg Germany, http://www.forwind.de/sowe/Site/Program_files/SOWE2013_Rahimi.pdf March 2013.

[5] "SIMPLE algorithm" http://www.cfd-online.com/Wiki/SIMPLE_algorithm, December 2011.

[6] D.K.Walters, D.Cokljat, "A three-Equation Eddy-Viscosity Model for Reynolds-Averaged Navier-Stokes Simulation of Transient Flow", December 2008.

[7] G.Eggenspieler "Turbulence Modeling" May 2012